

RESEARCH

Open Access



# Discovery and validation of a novel dual-target blood test for the detection of hepatocellular carcinoma across stages from cirrhosis

Wenhao Teng<sup>1,2†</sup>, Hui Li<sup>3,4†</sup>, Hao Yang<sup>4,5†</sup>, Yu Chen<sup>6</sup>, Liying Xi<sup>3,4</sup>, Fuli Xin<sup>1</sup>, Aiyuan Zhang<sup>3,4</sup>, Lihui Yu<sup>1</sup>, Lu Zheng<sup>3,4</sup>, Ming Wang<sup>1</sup>, Jian Bai<sup>3,4</sup>, Fayong Ke<sup>1</sup>, Yin Wang<sup>3,4</sup>, Fuming Sun<sup>4,5</sup>, Hui Zhang<sup>1\*</sup>, Lin Wu<sup>3,4\*</sup> and Jingfeng Liu<sup>1,4\*</sup>

## Abstract

**Background** Hepatocellular carcinoma (HCC) is one of the most common cancers. Early detection of HCC helps improve the patients' 5-year survival rate. Our goal was to identify superior methylation biomarkers to develop a methylation-specific quantitative PCR (MS-qPCR) assay.

**Methods** A five-phase case-control study identified HCC methylation biomarkers via capture sequencing, TCGA/RNA-seq filtering, technical (MS-qPCR/Sanger) and biological (quadruplex MS-qPCR) validation. Methylated biomarkers were selected based on differential methylation expression using a tissue discovery cohort (43 HCC, 32 normal) and validated in plasma validation cohorts (Phase 1: 53 HCC, 52 cirrhosis, 20 benign, 50 healthy; Phase 2: 67 HCC, 81 cirrhosis). Then, the final assay's HCC detection performance was compared with existing blood-based surveillance methods.

**Results** Two methylated genes, *OSR2* and *TSPYL5*, and a novel internal reference gene, *SDF4*, were identified and developed into an MS-qPCR assay named *Qliver*. *Qliver* had an AUC of 0.955 (95% CI: 0.924–0.987) for distinguishing HCC patients from non-HCC patients in the Phase 1 plasma cohort, with a sensitivity of 88.68% (95% CI: 76.97%–95.73%) and a specificity of 89.34% (95% CI: 82.47%–94.20%), and 0.958 (95% CI: 0.927–0.989) for distinguishing HCC patients from cirrhosis patients in the Phase 2 plasma cohort, with a sensitivity of 88.06% (95% CI: 77.82%–94.70%) and a specificity of 92.59% (95% CI: 84.57%–97.23%). For the Phase 1 plus Plasma 2 cohort, *Qliver* had an AUC of at least 0.958 for detecting HCC in healthy individuals, cirrhosis patients and patients with benign liver diseases, which was superior to that of the GALAD score (AUC: 0.777 to 0.849). For BCLC stage 0 and A HCC patients, the sensitivity of *Qliver* ranged from 62.50% (95% CI: 24.49%–91.48%) to 72.73% (39.03%–93.98%), with a specificity of 90%. Overall, *Qliver* was superior to the AFP, AFP-L3, DCP and the GALAD score in terms of cirrhosis history, tumor stage, tumor size and tumor count.

<sup>†</sup>Wenhao Teng, Hui Li and Hao Yang contributed equally to this work.

\*Correspondence:

Hui Zhang  
zh2405@hotmail.com

Lin Wu  
wulin@berryoncology.com

Jingfeng Liu  
drjingfeng@126.com

Full list of author information is available at the end of the article



**Conclusions** *Qliver* demonstrated superior performance in detecting HCC compared with currently widely used blood biomarkers, suggesting its potential clinical benefit in HCC surveillance in high-risk populations.

**Keywords** Hepatocellular carcinoma, DNA methylation, Early detection, Cirrhosis, Biomarker

## Background

Primary liver cancer is a common malignant tumor worldwide, ranking sixth in incidence and third in mortality among cancers [1]. Hepatocellular carcinoma (HCC) accounts for 75% to 85% of primary liver cancers [1]. HCC patients diagnosed at early stages can achieve a 70% 5-year survival rate through transplant or resection, whereas those with advanced HCC who are only eligible for palliative treatments have a medium survival rate of less than one year [2, 3]. Therefore, early detection of HCC can significantly improve patient survival rates. Liver ultrasound (US) is the recommended strategy for HCC surveillance in high-risk populations and is inexpensive but less effective in detecting early-stage HCC, with a sensitivity of 84% (95% confidence interval [CI]: 76%–92%) for any stage HCC detection, but only 47% (95% CI: 33%–61%) for early-stage HCC [4]. US performance depends on the examiner's experience, and obesity may further reduce its sensitivity [5]. Serum alpha-fetoprotein (AFP) is insufficient for screening for HCC, with a sensitivity of 25%–65% and a specificity of 80%–94% at a cutoff of 20 ng/mL, and only approximately 60%–80% of HCC patients have elevated AFP levels, resulting in a large margin for false negatives [6]. The sensitivity of combined US and AFP for detecting early HCC reached 63% (95% CI: 48%–75%) [4], but there is still room for improvement. The GALAD score, a blood biomarker-based model that combines age, sex,  $\alpha$ -fetoprotein (AFP), the lens culinaris agglutinin-reactive fraction of AFP (AFP-L3) and des-gamma-carboxyprothrombin (DCP), outperformed US in detecting early-stage HCC, with an AUC of 0.92 (95% CI: 0.88–0.96; cutoff: 1.18, sensitivity 92%, specificity 79%) [7]. Although the GALAD score performs well in the early detection of HCC, its performance still needs to be fully validated in the Chinese population, as chronic HBV infection is the main cause of HCC. Therefore, there is an urgent need for a noninvasive HCC detection method suitable for the Chinese population with high sensitivity and specificity.

DNA methylation is an epigenetic mechanism that regulates gene expression [8]. Hypermethylation of tumor suppressor genes is an early event in the carcinogenesis of many cancers [9, 10]. Circulating cell-free DNA (cfDNA) is an extracellular nucleic acid fragment released from necrotic, apoptotic or viable cells [11]. Circulating tumor DNA (ctDNA) originates from tumor cells and accounts for a small fraction of

cfDNA. Studies have shown that the methylation level of ctDNA in plasma is positively correlated with the number of primary tumor cells [12]. cfDNA methylation patterns have great potential as biomarkers for noninvasive cancer screening and monitoring [10, 13]. Guo et al. [14] developed a targeted methylation capture sequencing panel based on 283 CpG sites that has high accuracy in detecting HCC, with an AUC of 0.957 (sensitivity 90%, specificity 97%), but its workflow is cumbersome and costly. The use of a methylation-specific quantitative PCR (MS-qPCR) assay that combines two genes, *RNF135* and *LDHB*, is less expensive, but its performance in detecting HCC in high-risk groups (AUC=0.7306; 95% CI: 0.6955–0.7658) needs to be improved [15].

This study aimed to screen methylated genes with excellent performance, develop a cost-effective MS-qPCR assay for HCC detection, and validate its performance by comparing it with currently used biomarkers, including AFP, AFP-L3, DCP and the GALAD score.

## Methods

### Patient samples and characteristics

Patients aged 18 years or older with clinically diagnosed HCC in TNM stages I to III without treatment and individuals with liver cirrhosis or benign liver tumors such as hepatic adenomas, liver focal nodules or hepatic hemangiomas who were negative for HCC following disease surveillance were enrolled in the study. Twelve HCC patients with unknown TNM stage and 100 healthy volunteers without liver cirrhosis were also included. Frozen tissue and whole-blood samples from HCC patients and all non-HCC subjects and formalin-fixed paraffin-embedded (FFPE) slides from breast cancer and lung cancer patients were collected from Fujian Cancer Hospital. Whole blood samples of 8 to 10 mL were collected from each participant using Cell-Free DNA BCT<sup>®</sup> tubes (Streck, USA) and shipped to the laboratory at ambient temperature before plasma separation. Patient characteristics and demographic information are provided in Additional file 1: Table S1. All procedures were approved by Medical Ethics Committee of the Fujian Cancer Hospital (K2022-103-01). All research was conducted in accordance with the Declaration of Helsinki and the Declaration of Istanbul. Written consent was given by all the subjects.

### Study design

This study was conducted through five sequential case-control experiments (Fig. 1). A capture sequencing panel was employed to identify differentially methylated genes in tissue and validated in plasma samples from HCC patients and control subjects. These genes were then filtered through the TCGA 450 K and TCGA RNA-seq databases to select genes that exhibited high methylation in HCC samples and showed significant changes in RNA expression level compared with healthy. The selected genes were subsequently validated using MS-qPCR and Sanger sequencing with HCC tissues and adjacent normal tissues (ADJ) (tissue technical validation), and the top genes were chosen based on their differential methylation levels and haplotypes. Furthermore, the diagnostic performance of individual genes was assessed through biological validation using two quadruplex MS-qPCR assays in plasma from HCC patients, subjects with liver cirrhosis or benign liver diseases, and healthy individuals (Phase 1 plasma cohort), with the two genes exhibiting the best discriminative performance selected for the construction of the final assay. The diagnostic performance of this assay was subsequently validated using plasma obtained from HCC patients and subjects with liver cirrhosis (Phase 2 plasma cohort). Its diagnostic performance was then compared with that of existing blood biomarkers, including AFP, AFP-L3, DCP, and the GALAD score, across both the Phase 1 and Phase 2 plasma cohorts (see the Additional file 2 for details).

### Data analysis

#### Methylation profiling via targeted methylation sequencing

The FASTQ files were processed via the Cutadapt package (<https://github.com/marcelm/cutadapt/>) to obtain clean data by finding and removing adapter sequences and poly-tailed low-quality sequences and discarding reads shorter than 50 bp. Clean bisulfite reads were aligned to the hg19 human reference genome from the 1000 Genomes Phase 3 resources with decoy and patch sequences using BSMAP software (<https://code.google.com/archive/p/bsmap/>). The mapped reads were

split into top/bottom strands using bamtools software (<https://github.com/pezmaster31/bamtools>) according to the ZS tag in the BAM file generated by the BSMAP aligner, which indicated the top/bottom strands and the forward/reverse read status. Duplicates were removed separately by MarkDuplicates (Picard) (<https://github.com/broadinstitute/picard>), and the split files were rejoined and sorted by coordinates. ClipOverlap (bamUtil) (<https://github.com/statgen/bamUtil>) was used to prevent the converted/unconverted C bases in the overlapping regions from being double-counted. The percentage of methylated C bases was determined using the methratio.py script provided by BSMAP. BisMark (<https://github.com/FelixKrueger/Bismark>) was used to determine read-level cytosine methylation states (also known as the methylation haplotype).

#### Identification of informative CpG markers for HCC

HCC-specific informative CpG markers were identified using the following criteria: CpGs with more than 70% missing values in tissue or plasma samples were excluded during the tissue discovery and plasma validation phase. CpG retention with a  $P$  value  $< 0.01$  (two-sided Wilcoxon rank-sum test) was used to compare HCC tissues and adjacent normal tissues (ADJ). CpGs with a  $P$  value  $< 0.05$  (two-sided Wilcoxon rank-sum test) between plasma samples of patients with HCC and patients with liver cirrhosis and between plasma samples of patients with HCC and healthy controls were preserved. To identify differentially methylated CpGs, the methylation difference for each CpG was calculated as the mean methylation value of the HCC samples minus the mean methylation value of the control samples. CpGs with methylation differences  $\geq 0.3$ ,  $\geq 0.2$  and  $\geq 0.1$  in HCC tissues vs. ADJ tissues, HCC plasma vs. healthy subject plasma, and HCC plasma vs. liver cirrhosis plasma were filtered to retain CpGs with an FDR  $< 0.05$  (Student's two-sided  $t$  test and the Benjamini–Hochberg false discovery rate for  $P$  value correction). CpGs with median methylation levels  $\geq 40\%$  in HCC tissues and  $\geq 20\%$  in HCC plasma were retained. The removal of genes with stable expression levels,

(See figure on next page.)

**Fig. 1** Flow diagram to discovery and validation of a novel dual-targets blood test for detection of hepatocellular carcinoma across stages from cirrhosis patients. In tissue discovery cohort, we utilized a human methylome bisulfite panel which targets 123 Mb of genomic content to identify DNA methylation-based biomarkers starting with 43 primary HCC tissue and 32 adjacent normal tissue samples. 21 candidate markers were validated in 55 HCC, 55 cirrhosis and 50 healthy plasma samples by bisulfite sequencing in plasma discovery cohort. Technically validated methylated candidates were then biologically validated on 50 primary HCC tissue and 50 adjacent normal tissue samples (including tissue samples for tissue discovery) using methylation-specific quantitative PCR (MS-qPCR), yielding six candidate DNA markers for further validation. In phase 1 plasma cohort, candidate markers were validated in 53 HCC, 52 cirrhosis, 20 benign liver diseases and 50 healthy plasma samples. Two methylation genes, *OSR2* and *TSPYL5*, and a novel internal reference gene (*SDF4*) were identified, and an MS-qPCR assay named *Qliver* was constructed. An HCC detection model was trained using the relative methylation levels of *OSR2* and *TSPYL5*. Finally, *Qliver* model was further validated in 67 HCC and 81 cirrhosis plasma samples in phase 2 plasma cohort

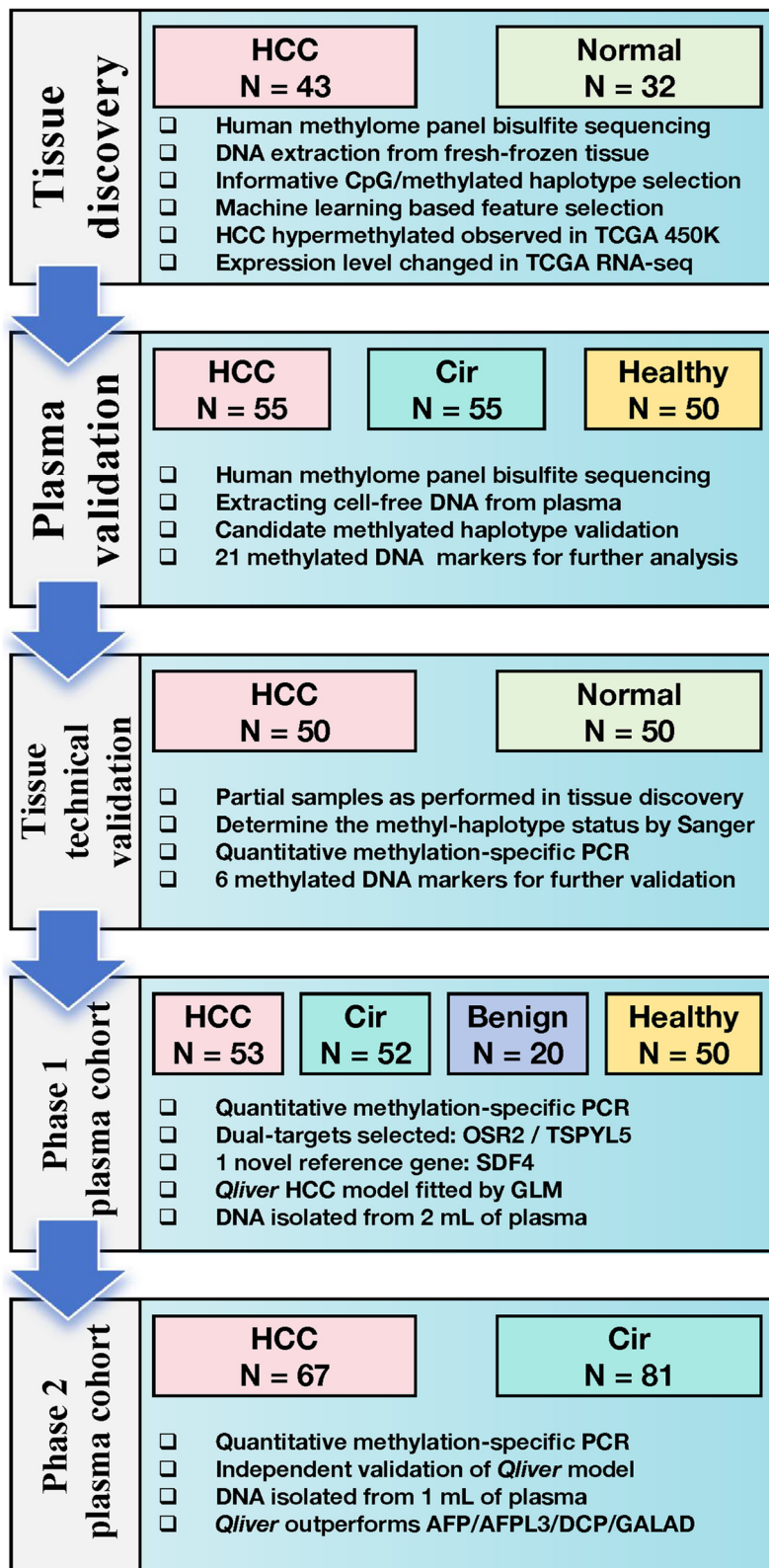


Fig. 1 (See legend on previous page.)

defined as a fold change between 0.95 and 1.05 between HCC patients and normal controls, was performed. This evaluation was based on RNA-Seq data obtained from the UCSC Xena Hub (<https://gdc.xenahubs.net>). Moreover, for dimensionality reduction and the selection of highly associated methylation features associated with hepatocellular carcinoma, the Boruta package ([https://github.com/scikit-learn-contrib/boruta\\_py](https://github.com/scikit-learn-contrib/boruta_py)) was utilized for feature selection to improve the performance of the model and resistant to overfitting and noise in the data.

### Identification of the methylated haplotype in HCC

In the aggregation step, neighboring informative CpGs with a predefined window size range (80–300 bp) were merged into candidate methylation haplotypes using a sliding window-based segmentation method. Three or more informative CpGs in each haplotype were required. Additionally, each identified haplotype had to be observed in sequencing reads from no fewer than 20 primary HCC tissues and 20 HCC plasma samples. The genes containing candidate methylation haplotypes were filtered using the TCGA 450 K dataset and TCGA RNA-Seq data. The genes with significantly higher methylation levels in HCC patients than in non-HCC individuals in the 450 K dataset but lower RNA expression levels in RNA-Seq data were retained because dysregulated DNA methylation can lead to the silencing of tumor suppressor genes or the expression of oncogenes, thus contributing to the development of cancer.

### Identification of a novel reference gene for MS-qPCR

Genes containing CpGs showing stable methylation levels were identified via the following criterion: exclusion of CpGs with more than 80% missing values in tissue samples. CpG methylation differences  $\leq 0.2$  were detected between HCC tissues and adjacent tissues, between HCC plasma samples and healthy plasma samples, and between HCC plasma samples and cirrhosis plasma samples. CpGs with median methylation levels  $\geq 60\%$  in HCC tissues and  $\geq 50\%$  in HCC plasma samples were retained. CpGs with a tau ( $\tau$ ) index  $\geq 0.05$  were removed from the analysis.

The tau ( $\tau$ ) index, which indicates whether a gene is tissue specific or ubiquitously methylated across tissues, produces a single specificity score for each gene or CpG site, indicating the ability to distinguish different cancer types from each other. The beta values of the DNA methylation 450 K array from the TCGA PanCan Atlas Cohort (9,639 samples across 32 tumor types) were downloaded and compiled by combining available data from all TCGA cohorts. The tau ( $\tau$ ) index was calculated as follows:

$$\tau = \frac{\sum_{i=1}^n 1 - \hat{x}_i}{n - 1}; \hat{x}_i = \frac{x_i}{\max_{1 \leq i \leq n} (x_i)}$$

where  $x_i$  is the beta value of the gene in cancer type  $i$  and  $n$  is the number of cancer types in the TCGA.  $\tau$  varies from 0 to 1, where 0 indicates consistent methylation levels across different tissues and 1 indicates tissue specificity.

Several steps were taken to refine the selection of candidate reference genes: the exclusion of genes containing CpG-SNP sites or with a low level of CpG density; the elimination of genes annotated as pseudogenes; and the removal of DEGs with expression fold changes  $> 1.05$  or  $< 0.95$  between patients with HCC and normal controls was performed. This evaluation was based on RNA-Seq data obtained from the UCSC Xena Hub (<https://gdc.xenahubs.net>).

### Statistical analysis

Candidate biomarker genes were selected based on the area under the receiver operating characteristic (ROC) curve (AUC) estimated using the R package pROC (version 1.18.0). The 95% confidence intervals (CIs) were calculated using 2000 stratified bootstrap replicates. A generalized linear model (GLM) was generated to analyze the correlations between the DNA methylation levels of selected genes based on the  $\Delta C_t$  values determined via MS-qPCR using the GLM function of R (4.1.1). All participants in phase 2 plasma cohort were random split into training and validate set with enough number of repeats ( $t=10$ ) and a reasonable balance between training and validate set (30% for training, 70% for validate). Comparing the difference ( $\Delta_{AUC}$ ) between the training and validation cohorts allows us to assess whether the difference is statistically significant, thereby evaluating the risk of overfitting.

### Sample size calculation

According to the literature and previous related studies, the expected sensitivity of the *Qliver* assay is 90% when the specificity is 90%. At a tolerance of 0.05 ( $\alpha=0.05$ ), at least 138 patients with HCC and 138 non-HCC participants were included in the pooled plasma cohort (Phase 1 plus Phase 2) according to the sample size ( $n$ ) calculation formula for diagnostic performance validation as follows [16]:

$$n = \frac{[Z_{1-\alpha/2}]^2 \times P \times (1 - P)}{\Delta^2}$$

where  $P$  is the predetermined value of the sensitivity (or specificity) that was ascertained from previously published data or clinician experience and for  $\alpha=0.05$

(meaning a 95% confidence level), and  $Z_{1-\alpha/2}$  is the standard normal variate (1.96 at 5% error).  $\Delta$  is the maximum marginal error of the estimate.

#### Performance calculation for an intended-use 10 K real-world population

The positive predictive value (PPV) of the *Qliver* assay and GALAD score (defined as the proportion of patients with HCC among participants with positive test results) were computed via Bayes' theorem as follows:

$$PPV = \frac{sensitivity \times prevalence}{sensitivity \times prevalence + (1 - specificity) \times (1 - prevalence)}$$

Similarly, the negative predictive value (NPV) of the *Qliver* assay and GALAD score (defined as the proportion of non-HCC subjects among participants with negative test results) were computed via Bayes' Theorem as follows:

$$NPV = \frac{specificity \times (1 - prevalence)}{(1 - sensitivity) \times prevalence + specificity \times (1 - prevalence)}$$

Similarly, positive predictive agreement (PPA) and negative predictive agreement (NPA) were computed as follows:

$$PPA = \frac{sensitivity \times prevalence}{sensitivity \times prevalence + (1 - specificity) \times (1 - prevalence) + (1 - sensitivity) \times prevalence}$$

$$NPA = \frac{specificity \times (1 - prevalence)}{(1 - sensitivity) \times prevalence + specificity \times (1 - prevalence) + (1 - specificity) \times (1 - prevalence)}$$

The benefit of using *Qliver* model to the intended-use population was evaluated as follows:

$$\frac{sensitivity}{1 - specificity} \geq \frac{1 - prevalence}{prevalence} \cdot \frac{harm}{benefit}$$

In particular, the incidence of HCC in the cirrhosis population is 2.1% per year according to R Fan et al. [17], which is an intended-use population.

#### Results

##### Identification of methylated genes and a novel internal reference gene for hepatocellular carcinoma detection

Through the analysis of methylation differences at indi-

vidual CpG sites in tissue and plasma samples, feature selection using machine learning, methylated haplotype identification and filtering through the TCGA database, we identified 21 candidate genes that exhibit highly methylation and linkage in hepatocellular carcinoma, includ-

ing *C1QL4*, *CR1L*, *CYP26C1*, *FOXG1*, *GHSR*, *HIST1H1D*, *IRX5*, *KCNG3*, *LHX2*, *MEX3A*, *NEFM*, *OSR2*, *OTX1*, *OXR*, *PCDHGB6*, *PCDHGB7*, *PITX1*, *PRLHR*, *PRRX1*,

*TSPYL5*, and *ZIC4*. The heatmap visually demonstrated that the methylation levels of these 21 genes were higher in HCC tissues than in adjacent normal tissues (Fig. 2A).

(See figure on next page.)

**Fig. 2** Identification of methylated markers for hepatocellular carcinoma. **A** Unclustered heatmap of the 21 most differentially methylated markers between 43 primary HCC and 32 adjacent normal tissue samples ( $p$ -value were computed with Wilcoxon rank sum test). **B** The distribution of methylation differential levels of 21 candidate markers in 55 HCC, 55 cirrhosis and 50 healthy plasma samples ( $p$ -value were computed with Wilcoxon rank sum test). Plasma\_Ctrl: cirrhosis and healthy plasma samples. Plasma\_HCC: HCC plasma samples **C** The distribution of  $\Delta$ CT value differences of 20 candidate markers (*OTX1* was excluded from the analysis due to nonspecific PCR amplification and primer-dimers) in 50 primary HCC and 50 adjacent normal tissue samples (including tissues for tissue discovery). HCC: hepatocellular carcinoma. ADJ: adjacent normal tissue. **D** ROC curves and associated AUC values with 95% confidential interval for six candidate DNA markers in 53 HCC, 52 cirrhosis, 20 benign liver disease and 50 healthy plasma samples. **E** Heatmap of methylation levels of CpGs in *OSR2* gene for discriminating Primary HCC tumor ( $n=377$ ), Recurrent HCC tumor ( $n=2$ ) and Solid Tissue Normal ( $n=50$ ) in the GDC TCGA Liver Cancer (LIHC) 450 K dataset. **F** Heatmap of methylation levels of CpGs in *TSPYL5* gene for discriminating Primary HCC tumor ( $n=377$ ), Recurrent HCC tumor ( $n=2$ ) and Solid Tissue Normal ( $n=50$ ) in the GDC TCGA Liver Cancer (LIHC) 450 K dataset. **G** The distribution of RNA expression values of *OSR2* and *TSPYL5* gene in Primary HCC tumor ( $n=377$ ), Recurrent HCC tumor ( $n=2$ ) and Solid Tissue Normal ( $n=59$ ) in the GDC TCGA Liver Cancer (LIHC) gene expression RNAseq dataset



Detailed information on the methylation blocks of the 21 candidate genes is summarized in Additional file 1: Table S2.

Among the 21 candidate genes, six genes, namely, *KCNKG3* ( $p=4.4e-11$ ), *OSR2* ( $p=5.9e-09$ ), *IRX5* ( $p=8.8e-08$ ), *PITX1* ( $p=2.3e-08$ ), *OTX1* ( $p=4.7e-08$ ), and *TSPYL5* ( $p=1.1e-08$ ), presented the most significant differences in methylation levels in plasma samples from HCC patients, subjects with liver cirrhosis and healthy individuals (Fig. 2B). Moreover, the methylation profiles of 43 primary HCC tissues and 32 adjacent normal tissues revealed that these six genes exhibited HCC-specific methylation haplotypes (Additional file 3: Fig. S1). These results suggest that these 21 genes have great potential in HCC detection, especially these 6 genes.

Several steps were undertaken to refine the selection of candidate reference genes, as mentioned in the [Methods](#) section. Ultimately, *UBE2K*, *SDF4*, *PIGG* and *KIAA0562* were selected as candidate reference genes. Homo sapiens stromal cell-derived factor 4 (*SDF4*), which encodes a stromal cell-derived factor that is a member of the CREC protein family, was ultimately identified in an independent pilot experiment as the most stably conserved reference gene in the tissue and plasma of patients with HCC and control subjects. *SDF4* gene was hypermethylated in both HCC tissues and adjacent normal tissues and that the methylation levels of its hypermethylated chromosomal regions were not significantly different between HCC tissues and adjacent normal tissues (Additional file 3: Fig. S2). We also observed from the GDC TCGA Liver Cancer (LIHC) 450 K database that most CpG sites in the *SDF4* gene are hypermethylated in HCC primary tumor tissues, normal solid tissues, and recurrent HCC tissues (Additional file 3: Fig. S3A). According to the GDC PanCancer (PANCAN) 450 K dataset, the methylation levels of most CpG sites in the *SDF4* gene did not differ significantly between different cancer types (Additional file 3: Fig. S3G). The results of capture sequencing

and public database analysis revealed that *SDF4* could be used as an internal reference gene for MS-qPCR because of its stable high methylation level.

#### Technical validation of methylated genes and internal reference gene

The 21 candidate genes were technically validated in 50 HCC tissues and 50 adjacent normal tissues via MS-qPCR to screen out several more reliable genes. *OTX1* was excluded from the MS-qPCR validation because of nonspecific amplification and a high proportion of primer dimers. The differences in the methylation of *OSR2* ( $p=5.2e-11$ ), *CIQL4* ( $p=2.2e-11$ ), *PITX1* ( $p=1.4e-10$ ), *KCNKG3* ( $p=1.2e-10$ ), *IRX5* ( $p=5.4e-09$ ), *TSPYL5* ( $p=8.2e-08$ ), *ZIC4* ( $p=3.4e-08$ ) and *FOXP1* ( $p=1.8e-08$ ) were more significant than those of the other 12 genes (Fig. 2C). Sanger sequencing was performed on tissue samples to confirm the methylation linkage status of the candidate genes. The methylation levels of the CpG sites of the *OSR2* and *TSPYL5* genes in HCC tissues were significantly greater than those in adjacent normal tissues, and most of these CpGs were comethylated (Additional file 3: Fig. S4). On the basis of the  $p$  values from low to high, we selected the top six genes, namely, *OSR2*, *CIQL4*, *PITX1*, *KCNKG3*, *IRX5* and *TSPYL5*, for biological validation in independent plasma samples by two quadruplex MS-qPCR.

In addition, the potential of the *SDF4* gene as an internal reference was further verified using genomic DNA from leukocytes and tissues, as well as plasma cfDNA, in comparison with the commonly used internal reference gene *ACTB*. The Ct values of MS-qPCR for *SDF4* and *ACTB* were moderately correlated with the input amount of leukocyte genomic DNA (Additional file 3: Fig. S3E, F). There was no significant difference in the Ct values of *SDF4* between 38 primary HCC tissues and 38 adjacent normal tissues (Additional file 3: Fig. S3C) or between 12 breast cancer tissues and 20 lung cancer

(See figure on next page.)

**Fig. 3** Construction and validation the diagnostic performance of *Qliver* model to detect HCC in plasma cohort. **A** 2D kernel density estimation of  $\Delta$ CT value of *OSR2* and *TSPYL5* gene in combined plasma cohort (phase 1 plus phase 2), which consists with 120 HCC, 133 cirrhosis, 20 benign liver disease and 50 healthy plasma samples. **B** ROC curves and associated AUC values for *OSR2*, *TSPYL5*, AFP, AFP-L3, DCP, GALAD and *Qliver* in phase 1 plasma cohort consisting of 53 HCC, 52 cirrhosis, 20 benign liver disease and 50 healthy plasma samples. **C** ROC curves and associated AUC values for *OSR2*, *TSPYL5*, AFP, AFP-L3, DCP, GALAD and *Qliver* in phase 2 plasma cohort consisting of 67 HCC and 81 cirrhosis plasma samples. **D** The comparison of  $\Delta$ CT values of *OSR2* (**D**), *TSPYL5* (**E**), *Qliver* score (**F**) and GALAD score (**G**) in different sample groups in combined plasma cohort (phase 1 plus phase 2), consisting of 120 HCC, 133 cirrhosis, 20 benign liver disease and 50 healthy plasma samples ( $p$ -value were computed with Wilcoxon rank sum test). \*,  $p < 0.05$ ; \*\*,  $p < 0.01$ ; \*\*\*,  $p < 0.001$ ; \*\*\*\*,  $p < 0.0001$ ;  $p > 0.05$  was considered not significant (ns). Healthy, healthy volunteers; HCA, Hepatocellular adenoma; FNH, Focal Nodular Hyperplasia; HH, Hepatic hemangioma; Cir, liver cirrhosis; HCC, hepatocellular carcinoma. **H** Comparison of HCC prediction results between *Qliver* and other classifiers in combined plasma cohort (phase 1 plus phase 2) consisting of 120 HCC, 133 cirrhosis, 20 benign liver diseases and 50 healthy plasma samples. A Z-score normalization is performed on the normalized value across samples for each marker. Heatmaps and dendrograms were also created to depict the *Qliver* characteristics based on the Euclidean distance and ward. D2 clustering methods. Since *OSR2* and *TSPYL5* are highly methylated in HCC patients, the  $\Delta$ ct value of their MS-qPCR amplification is lower than that of the control subjects

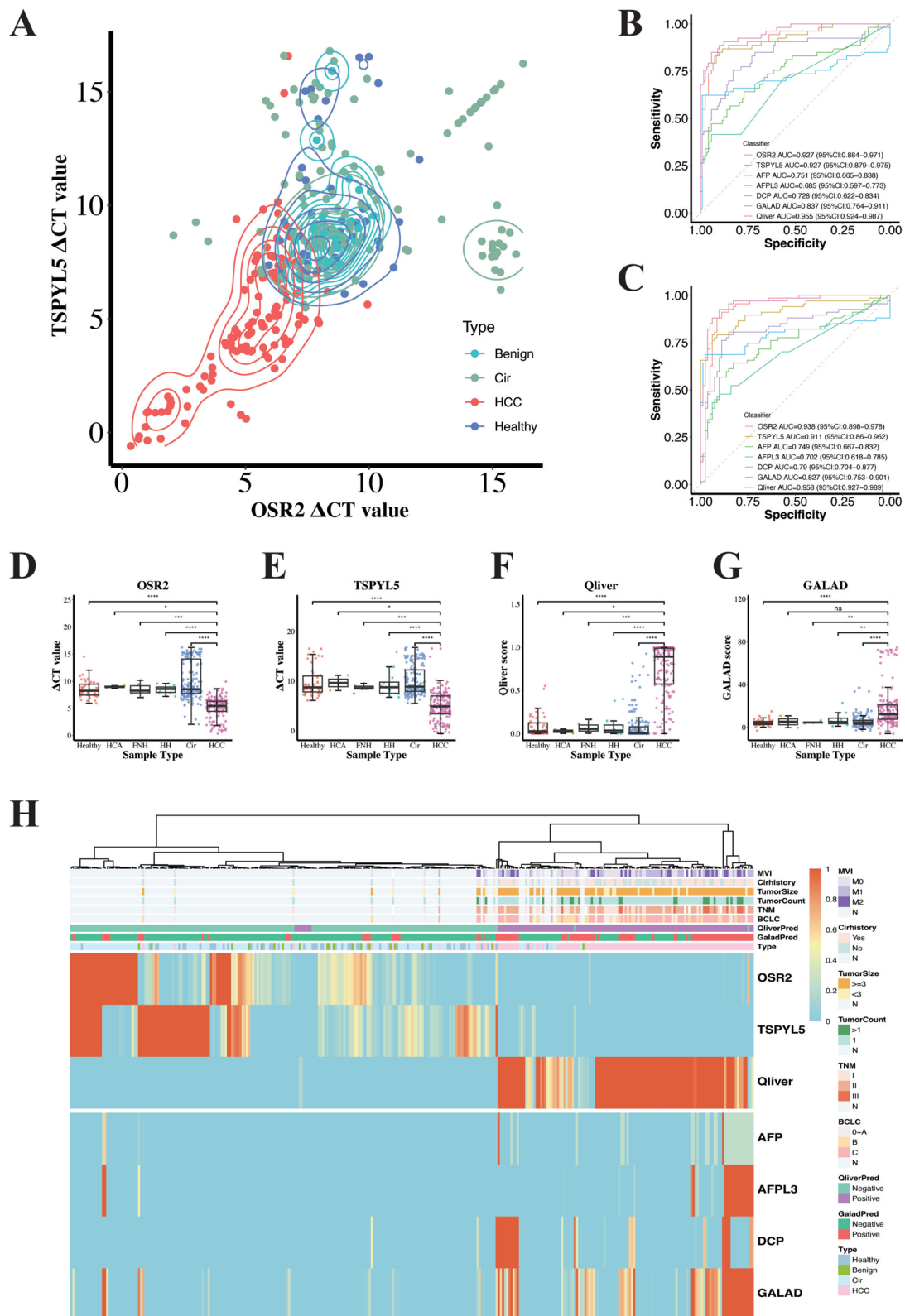


**Fig. 3** (See legend on previous page.)

FFPE tissues (Additional file 3: Fig. S3D), and the same was true for *ACTB*. However, *SDF4* was amplified more efficiently than *ACTB*. Importantly, when *SDF4* was used as an internal reference gene, the hypermethylated gene *ZIC4* performed better in distinguishing HCC patients, cirrhosis patients, and healthy controls than when *ACTB* was used as an internal reference gene in 2 mL plasma samples (AUC 0.826, 95% CI: 0.664–0.988 vs. AUC 0.786, 95% CI: 0.608–0.964) (Additional file 3: Fig. S3B).

#### Establishment of *Qliver* score in 2 mL plasma cohort

The six candidate genes were validated by two quadruplex MS-qPCR using *SDF4* as an internal reference gene in an independent set of plasma samples (Phase 1 plasma cohort), which included 53 HCC patients, 52 cirrhosis patients, 20 individuals with benign liver diseases and 50 healthy volunteers. Subsequently, the six candidate genes were combined in pairs, and their diagnostic performance for HCC detection was evaluated. The combination of *OSR2* and *TSPYL5* exhibited the highest diagnostic performance (AUC = 0.955, 95% CI: 0.924–0.987) (Additional file 1: Table S3), outperforming either gene individually (*OSR2*: AUC = 0.927, 95% CI: 0.884–0.971; *TSPYL5*: AUC = 0.927, 95% CI: 0.879–0.975), highlighting their potential as optimal methylation markers for HCC detection (Fig. 2D).

Subsequently, an MS-qPCR assay named *Qliver*, which includes *OSR2*, *TSPYL5* and *SDF4*, was developed for HCC detection. The *Qliver* score, which represents the probability of a subject having HCC, was calculated according to the following formula generated by the GLM:

$$Qliverscore = 1 - \frac{1}{1 + e^{11.608 - 0.882 * \Delta_{OSR2} - 0.835 * \Delta_{TSPYL5}}}$$

where *e* is Euler's number, a mathematical constant approximately equal to 2.71828;

$\Delta_{OSR2}$  refers to the  $\Delta$ Ct value of *OSR2*, which is obtained by subtracting the Ct value of *SDF4* from the Ct value of *OSR2*;

$\Delta_{TSPYL5}$  refers to the  $\Delta$ Ct value of *TSPYL5*, which is obtained by subtracting the Ct value of *SDF4* from the Ct value of *TSPYL5*.

The  $\Delta$ Ct values of *OSR2* and *TSPYL5* in the Phase 1 plasma cohort were trained to construct a model (*Qliver* model) for predicting HCC using the generalized linear model (GLM), and the performance of *Qliver* was compared with that of protein biomarkers, such as AFP, AFP-L3, DCP and the GALAD score. The coefficients and intercept of the GLM of the *Qliver* model are shown in Additional file 1: Table S4. The AUC of *Qliver* for distinguishing HCC patients from non-HCC patients was 0.955 (95% CI: 0.924–0.987), which was significantly greater

than that of AFP (0.751, 95% CI: 0.665–0.838), AFP-L3 (0.685, 95% CI: 0.597–0.773), DCP (0.728, 95% CI: 0.622–0.834), and the GALAD score (0.837, 95% CI: 0.764–0.911; *P* value = 0.003, DeLong's test). Even the AUCs of the single genes *OSR2* (0.927, 95% CI: 0.884–0.971) and *TSPYL5* (0.927, 95% CI: 0.879–0.975) were greater than those of the GALAD score when multiple protein markers were combined (Fig. 3B). When the specificity was set at almost the same level (85.25%–89.34%), the sensitivity of *Qliver* for distinguishing HCC patients from non-HCC patients was 88.68% (95% CI: 76.97%–95.73%), which was better than that of AFP (47.17, 95% CI: 33.30%–61.36%), AFP-L3 (41.51%, 95% CI: 28.14%–55.87%), DCP (62.26%, 95% CI: 47.89%–75.21%) and the GALAD score (58.49%, 95% CI: 44.13%–71.86%) (Table 1). The PPV of *Qliver* for detecting HCC in non-HCC patients was 78.33% (95% CI: 68.19%–85.91%), which was significantly greater than that of AFP (65.79%, 95% CI: 51.66%–77.58%), AFP-L3 (57.89%, 95% CI: 44.05%–70.60%), DCP (64.71%, 95% CI: 53.27%–74.68%) and the GALAD score (70.45%, 95% CI: 57.62%–80.70%). The NPV of *Qliver* for detecting HCC in non-HCC patients was 94.78% (95% CI: 89.51%–97.48%), which was significantly greater than that of AFP (79.56%, 95% CI: 74.98%–83.49%), AFP-L3 (77.37%, 95% CI: 72.96%–81.25%), DCP (83.87%, 95% CI: 78.50%–88.10%) and the GALAD score (83.21%, 95% CI: 78.16%–87.28%) (Table 1).

With a specificity of 90%, *Qliver* was more sensitive than AFP, AFP-L3, DCP and the GALAD score in detecting all stages (BCLC stage) of HCC. In particular, the sensitivity of *Qliver* in detecting stage 0 + A HCC was 62.50% (95% CI: 24.49%–91.48%), which was significantly greater than that of AFP (37.50%, 95% CI: 8.52%–75.51%), AFP-L3 (50.00%, 95% CI: 15.70%–84.30%), DCP (25.00%, 95% CI: 3.19%–65.09%) and the GALAD score (25.00%, 3.19%–65.09%) (Table 2). Moreover, *Qliver* was more specific than these protein biomarkers in detecting hepatic adenomas and hemangiomas (Additional file 1: Table S5). A more detailed comparison of *Qliver* with the protein biomarkers is shown in Additional file 1: Table S5.

#### Stable performance of *Qliver* score in independent 1 mL plasma cohort

The *Qliver* model was further validated in an additional independent cohort of plasma samples (Phase 2 plasma cohort), with the volume of each plasma sample reduced from 2 to 1 mL. The AUC of *Qliver* (0.958, 95% CI: 0.927–0.989) in distinguishing 67 HCC patients from 81 patients with liver cirrhosis was significantly greater than that of AFP (0.749, 95% CI: 0.667–0.832), AFP-L3 (0.702, 95% CI: 0.618–0.785), DCP (0.790, 95% CI: 0.704–0.877), and the GALAD score (0.827, 95% CI: 0.753–0.901; *P* value = 0.001, DeLong's test). Even the AUCs of the single

**Table 1** HCC detection metrics of *Qliver*, AFP, AFP-L3, DCP, and GALAD score

Cohort	Model	Sensitivity(%) (95%CI)	Specificity(%) (95%CI)	PPV(%) (95%CI)	NPV(%) (95%CI)
Phase 1 plasma cohort	<i>Qliver</i>	88.68 (76.97–95.73) [47/53]	89.34 (82.47–94.20) [109/122]	78.33 (68.19–85.91) [47/60]	94.78 (89.51–97.48) [109/115]
	AFP	47.17 (33.30–61.36) [25/53]	89.34 (82.47–94.20) [109/122]	65.79 (51.66–77.58) [25/38]	79.56 (74.98–83.49) [109/137]
	AFPL3	41.51 (28.14–55.87) [22/53]	86.89 (79.58–92.31) [106/122]	57.89 (44.05–70.60) [22/38]	77.37 (72.96–81.25) [106/137]
	DCP	62.26 (47.89–75.21) [33/53]	85.25 (77.69–91.02) [104/122]	64.71 (53.27–74.68) [33/51]	83.87 (78.50–88.10) [104/124]
	GALAD	58.49 (44.13–71.86) [31/53]	89.34 (82.47–94.20) [109/122]	70.45 (57.62–80.70) [31/44]	83.21 (78.16–87.28) [109/131]
Phase 2 plasma cohort	<i>Qliver</i>	88.06 (77.82–94.70) [59/67]	92.59 (84.57–97.23) [75/81]	90.77 (81.92–95.52) [59/65]	90.36 (82.99–94.74) [75/83]
	AFP	50.75 (38.24–63.18) [34/67]	90.12 (81.46–95.64) [73/81]	80.95 (67.88–89.53) [34/42]	68.87 (63.19–74.03) [73/106]
	AFPL3	47.76 (35.40–60.33) [32/67]	83.95 (74.12–91.17) [68/81]	71.11 (58.50–81.13) [32/45]	66.02 (60.26–71.34) [68/103]
	DCP	68.66 (56.16–79.44) [46/67]	76.54 (65.82–85.25) [62/81]	70.77 (61.27–78.74) [46/65]	74.70 (67.00–81.11) [62/83]
	GALAD	59.70 (47.00–71.51) [40/67]	91.36 (83.00–96.45) [74/81]	85.11 (73.26–92.26) [40/47]	73.27 (67.02–78.71) [74/101]
Intended-use 10 K population <sup>a</sup>	<i>Qliver</i>	88.10 (82.93–92.15) [185/210]	92.59 (92.06–93.11) [9065/9790]	20.33 (18.97–21.76) [185/910]	99.72 (99.60–99.81) [9065/9090]
	AFP	50.95 (43.98–57.90) [107/210]	90.12 (89.51–90.71) [8823/9790]	9.96 (8.73–11.35) [107/1074]	98.85 (98.68–98.99) [8823/8926]
	AFPL3	47.62 (40.70–54.60) [100/210]	83.95 (83.21–84.68) [8219/9790]	5.98 (5.20–6.88) [100/1671]	98.68 (98.50–98.84) [8219/8329]
	DCP	68.57 (61.82–74.79) [144/210]	76.54 (75.68–77.37) [7493/9790]	5.90 (5.38–6.47) [144/2441]	99.13 (98.94–99.28) [7493/7559]
	GALAD	59.52 (52.55–66.22) [125/210]	91.36 (90.78–91.91) [8944/9790]	12.87 (11.50–14.39) [125/971]	99.06 (98.89–99.20) [8944/9029]

<sup>a</sup> HCC incidence is 2.1% per year in cirrhotic population according our previous study<sup>9</sup>, which is an intended-use population of *Qliver*

genes *OSR2* (0.938, 95% CI: 0.898–0.978) and *TSPYL5* (0.911, 95% CI: 0.860–0.962) were greater than those of the GALAD score (Fig. 3C). When the specificity was set at 90.12–92.59%, the sensitivity of *Qliver* (88.06%, 95% CI: 77.82%–94.70%) for detecting HCC was greater than that of AFP (50.75%, 95% CI: 38.24%–63.18%) and the GALAD score (59.70%, 95% CI: 47.00%–71.51%). The sensitivity and specificity of *Qliver* were both greater than those of AFP-L3 (47.76%, 95% CI: 35.40%–60.33%; 83.95%, 95% CI: 74.12%–91.17%) and DCP (68.66%, 95% CI: 56.16%–79.44%; 76.54%, 95% CI: 65.82%–85.25%) (Table 1). The PPV (90.77%, 95% CI: 81.92%–95.52%) and NPV (90.36%, 95% CI: 82.99%–94.74%) of *Qliver* were both greater than those of the GALAD score (85.11%, 95% CI: 73.26%–92.26%; 73.27%, 95% CI: 67.02%–78.71%) and other protein biomarkers (Table 1).

When the plasma volume was reduced to 1 mL, *Qliver* still performed better than the other biomarkers in detecting early-stage HCC. For stage 0+A stage HCC patients, the sensitivity of *Qliver* was 72.73% (95% CI:

39.03%–93.98%), whereas those of AFP, AFP-L3, DCP and the GALAD score were 9.09% (95% CI: 0.23%–41.28%), 18.18% (95% CI: 2.28%–51.78%), 54.55% (95% CI: 23.38%–83.25%) and 18.18% (95% CI: 2.28%–51.78%), respectively. For stage B and C HCC, the sensitivity of *Qliver* was still greater than those of these protein markers (Table 2). A comparison of biomarker performance in the Phase 2 plasma cohort is detailed in Additional file 1: Table S5.

#### ***Qliver* outperforms protein biomarkers in the combined cohort**

The MS-qPCR data of the *OSR2* and *TSPYL5* genes from the Phase 1 plasma cohort were combined with those from the Phase 2 plasma cohort to further evaluate the performance of *Qliver* in detecting HCC in a larger sample size. The  $\Delta\text{Ct}$  values of *OSR2* and *TSPYL5* were clearly clustered into two large groups between the HCC patients ( $n=120$ ) and the non-HCC controls ( $n=203$ ) (Fig. 3A). In the combined plasma cohort, the  $\Delta\text{Ct}$

**Table 2** Sensitivity for the HCC detection of *Qliver*, AFP, AFP-L3, DCP, and GALAD score across BCLC stages

Cohort	Model	BCLC Stage		
		0 + A	B	C
Phase 1 plasma cohort	<i>Qliver</i>	62.50 (24.49–91.48) [5/8]	85.71 (57.19–98.22) [12/14]	96.77 (83.30–99.92) [30/31]
	AFP	37.50 (8.52–75.51) [3/8]	28.57 (8.39–58.10) [4/14]	58.06 (39.08–75.45) [18/31]
	AFPL3	50.00 (15.70–84.30) [4/8]	28.57 (8.39–58.10) [4/14]	45.16 (27.32–63.97) [14/31]
	DCP	25.00 (3.19–65.09) [2/8]	71.43 (41.90–91.61) [7/14]	67.74 (48.63–83.32) [22/31]
	GALAD	25.00 (3.19–65.09) [2/8]	50.00 (23.04–76.96) [7/14]	70.97 (51.96–85.78) [22/31]
Phase 2 plasma cohort	<i>Qliver</i>	72.73 (39.03–93.98) [8/11]	95.45 (77.16–99.88) [21/22]	88.24 (72.55–96.70) [30/34]
	AFP	9.09 (0.23–41.28) [1/11]	54.55 (32.21–75.61) [21/22]	61.76 (43.56–77.83) [30/34]
	AFPL3	18.18 (2.28–51.78) [2/11]	54.55 (32.21–75.61) [12/22]	52.94 (35.13–70.22) [18/34]
	DCP	54.55 (23.38–83.25) [6/11]	68.18 (45.13–86.14) [15/22]	73.53 (55.64–87.12) [25/34]
	GALAD	18.18 (2.28–51.78) [2/11]	68.18 (45.13–86.14) [15/22]	67.65 (49.47–82.61) [23/34]
Combined plasma cohort	<i>Qliver</i>	68.42 (43.45–87.42) [13/19]	91.67 (77.53–98.25) [33/36]	92.31 (82.95–97.46) [60/65]
	AFP	21.05 (6.05–45.57) [4/19]	44.44 (27.94–61.90) [16/36]	60.00 (47.10–71.96) [39/65]
	AFPL3	31.58 (12.58–56.55) [6/19]	44.44 (27.94–61.90) [16/36]	49.23 (36.60–61.93) [32/65]
	DCP	42.11 (20.25–66.50) [8/19]	69.44 (51.89–83.65) [25/36]	70.77 (58.17–81.40) [46/65]
	GALAD	21.05 (6.05–45.57) [4/19]	61.11 (43.46–76.86) [22/36]	69.23 (56.55–80.09) [45/65]

Cutoff defined at specificity 90% in phase 1 plasma cohort

values of *OSR2* and *TSPYL5* in the HCC patients were significantly lower than those in the non-HCC patients ( $p < 0.05$ ) (Fig. 3D, E). The *Qliver* score and the GALAD score of the HCC patients were both significantly greater than those of the healthy volunteers, patients with focal nodular hyperplasia (FNH), patients with hepatic hemangioma (HH) and cirrhosis patients (Cir) ( $p < 0.05$ ), but *Qliver* performed better overall (Fig. 3F, G). There was a significant difference in the *Qliver* score, but not the GALAD score, between HCC patients and patients with hepatocellular adenoma (HCA) (Fig. 3F, G).

The sensitivity of *Qliver* in detecting HCC at BCLC stages 0 and A was 68.42% (95% CI: 43.45%–87.42%), which was superior to that of the GALAD score at 21.05% (95% CI: 6.05%–45.57%) (Table 2). Similar results were observed in other BCLC stages.

The AUC of *Qliver* was greater than that of the GALAD score in distinguishing HCC patients from healthy volunteers, cirrhosis patients, and individuals

with benign liver disease (0.958, 95% CI: 0.934–0.983 vs. 0.849, 95% CI: 0.797–0.901;  $P < 0.001$ ; 0.958, 95% CI: 0.938–0.978 vs. 0.810, 95% CI: 0.761–0.858,  $P < 0.001$ ; 0.959, 95% CI: 0.930–0.988 vs. 0.777, 95% CI: 0.679–0.874,  $P < 0.001$ ; DeLong's test) (Fig. 4A–C). Similar results were observed for AFP, AFP-L3 and DCP. For single-gene comparisons, *OSR2* performed better than *TSPYL5*.

The sensitivity and specificity of *Qliver* for detecting HCC were greater than those of AFP, AFP-L3, DCP and the GALAD score in patients with different liver cirrhosis histories, tumor sizes, tumor counts and tumor stages (Fig. 3H). The positive rate of *Qliver* in detecting HCC was higher than that of the GALAD score under different AFP and DCP concentrations, BCLC stages, liver cirrhosis histories, maximum tumor sizes and tumor counts (Fig. 4D–I). A detailed performance comparison of *Qliver* with these biomarkers in the combined plasma cohort is shown in Additional file 1: Table S5.

### Evaluating the benefit of *Qliver* score for a 10 K intended-use population

To evaluate the performance of *Qliver* in the real world, a population of 10,000 cirrhosis patients was simulated. When the annual incidence of HCC was 2.1%, the PPV and NPV of *Qliver* were 20.33% (95% CI: 18.97%–21.76%) and 99.72% (95% CI: 99.60%–99.81%), respectively, which were higher than those of the GALAD score (12.87%, 95% CI: 11.50%–14.39%; 99.06%, 95% CI: 98.99%–99.20%) (Table 1). In addition, the PPV of *Qliver* was significantly greater than those of AFP, AFP-L3 and DCP.

The benefit of using the *Qliver* model for the intended user population was evaluated. When the prevalence of HCC in the cirrhotic population was 2.1%, the sensitivity of *Qliver* for detecting HCC was 88.33%, and the specificity was 90.64%, the harm/benefit ratio was  $\leq 0.2024273$ , which means that in order to benefit one *Qliver*-positive case subject, 5 *Qliver*-positive control subjects should be tolerated to undergo unnecessary clinical measures such as ultrasound examination.

### Potential application of *Qliver* score in HCC prognosis

The potential of *Qliver* in HCC prognosis was also explored in this study. By analyzing the GDC TCGA Liver Cancer (LIHC) 450 K dataset, we found that the methylation levels of some CpG sites in *OSR2* and most CpG sites in *TSPYL5* were greater in primary HCC tumors ( $n=377$ ) and recurrent tumors ( $n=2$ ) than in normal solid tissues ( $n=59$ ) (Fig. 2E, F). According to the GDC TCGA Liver Cancer (LIHC) gene expression RNA-seq dataset, the mRNA expression level of *OSR2* in primary HCC tumors ( $n=377$ ) and recurrent HCC tumors ( $n=2$ ) was significantly greater than that in normal solid tissues ( $n=59$ ). However, the opposite results were observed for *TSPYL5* (Fig. 2G).

The disease-free survival (DFS) of 365 HCC patients in the GDC TCGA Liver Cancer (LIHC) 450 K dataset was evaluated on the basis of the methylation levels of the *OSR2* and *TSPYL5* genes. Patients with higher *OSR2* methylation levels had significantly worse DFS than those

with lower methylation levels, with a hazard ratio (HR) of 1.393 (95% CI: 1.028–1.888) ( $p=0.029$ ; log-rank test) (Fig. 4J). However, there was no significant difference in DFS between HCC patients with high and low *TSPYL5* methylation levels, with an HR of 1.317 (95% CI: 0.974–1.781) ( $p=0.072$ ; log-rank test) (Fig. 4K). Nevertheless, the DFS of HCC patients with high dual-gene methylation levels was significantly lower than that of patients with low dual-gene methylation levels. Moreover, double gene methylation was better than single gene methylation in predicting prognosis ( $p=0.008$ ; log-rank test, HR=1.627, 95% CI: 1.127–2.350) (Fig. 4L). These findings indicate that hypermethylated *OSR2* and *TSPYL5* are promising markers for HCC prognosis.

Patients with higher methylation levels of *OSR2* or *TSPYL5* gene had a significantly lower DFS rate than those with low methylation levels across different age or AJCC stage. Moreover, combining the *TSPYL5* and *OSR2* genes, the DFS rate of HCC patients with high methylation levels of both genes was significantly lower than that of patients with low methylation levels (Additional file 3: Fig. S5).

### Potential application of *Qliver* score in multi-cancer detection

The methylation levels of *OSR2* and *TSPYL5* were validated in multiple tumor cell lines and white blood cells (WBCs). The methylation levels of the *OSR2* gene were significantly greater in most tumor cell lines than in leukocytes, especially in CAL-62 (thyroid), HCC-2279 (lung), MKN74 (stomach), MKN28 (stomach), EFM-19 (breast) and MCF7 (breast) cells (Additional file 3: Fig. S6). This finding suggests that the *OSR2* gene may be an oncogene, so *Qliver* can be used for multicancer detection.

### Discussion

Early detection is crucial for improving the 5-year survival rate of patients with various cancers, including liver cancer [18]. In this study, we identified two methylated

(See figure on next page.)

**Fig. 4** Comparison of the performance of *Qliver* and GALAD score in different subgroups and the possibility of using *Qliver* for HCC prognosis.

**A** ROC curves and associated AUC values with 95% confidential interval for *OSR2*, *TSPYL5*, AFP, AFP-L3, DCP, GALAD and *Qliver* in combined plasma cohort (phase 1 plus phase 2) consisting of 120 HCC and 50 healthy plasma samples. **B** ROC curves and associated AUC values with 95% confidential interval for *OSR2*, *TSPYL5*, AFP, AFP-L3, DCP, GALAD and *Qliver* in combined plasma cohort consisting of 120 HCC and 50 cirrhosis plasma samples. **C** ROC curves and associated AUC values with 95% confidential interval for *OSR2*, *TSPYL5*, AFP, AFP-L3, DCP, GALAD and *Qliver* in combined plasma cohort, consisting of 120 HCC and 20 benign liver disease samples. **D** Comparison of positive and negative proportions of HCC detection by *Qliver* and GALAD score in HCC patients ( $n=120$ ) at different AFP concentrations. ( $< 20 \mu\text{g/L}$ ,  $20 \mu\text{g/L} \leq \text{AFP} \leq 400 \mu\text{g/L}$ ,  $> 400 \mu\text{g/L}$ ), **E** at different DCP concentrations ( $D < 40\text{mAU/mL}$ , and  $\geq 40\text{mAU/mL}$ ), **F** at BCLC 0/A/B/C stages, **G** at different cirrhosis history, **H** at different tumor size and **(I)** at different tumor count. Kaplan–Meier estimates of disease-free survival in HCC patients ( $n=365$ ) in the GDC TCGA Liver Cancer (LIHC) 450 K dataset, stratified by methylation level of *OSR2* gene **(J)**, *TSPYL5* gene **(K)** and dual-target **(L)**. The DFS outcomes between  $OSR2_{\text{high}}/TSPYL5_{\text{high}}$  and  $OSR2_{\text{low}}/TSPYL5_{\text{low}}$  groups were compared using the log-rank test

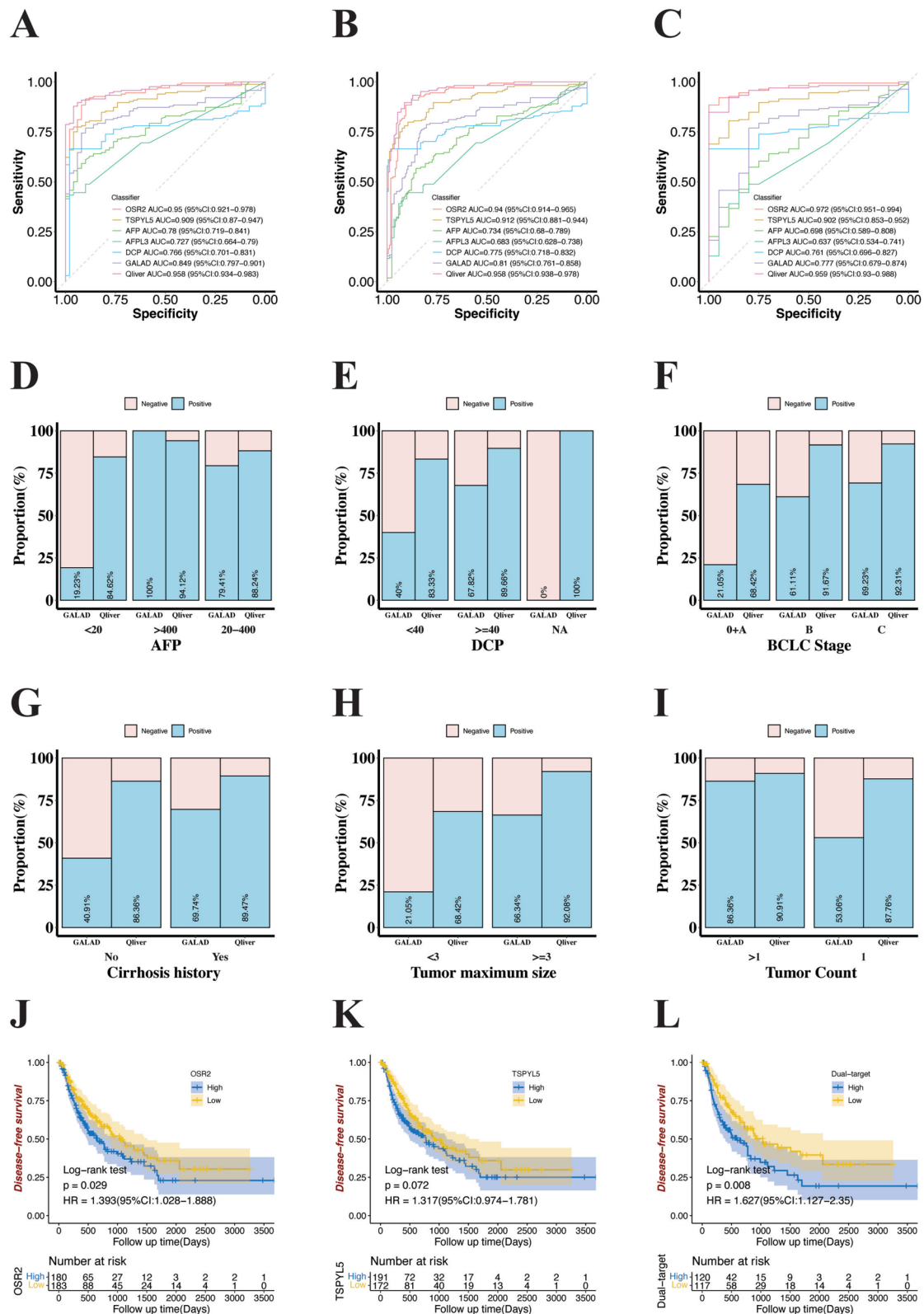


Fig. 4 (See legend on previous page.)

genes, *OSR2* and *TSPYL5*, for HCC detection and developed an MS-qPCR assay named *Qliver*. We compared the performance of *Qliver* for detecting HCC with that of existing surveillance methods with respect to cirrhosis history, tumor size, tumor count, and tumor stage. *Qliver* performed best in HCC detection, followed by the GALAD score. The performance of *Qliver* far exceeded that of AFP, AFP-L3 and DCP. In cirrhosis patients, subjects with benign liver diseases and healthy individuals as controls, the pooled sensitivity of *Qliver* for detecting HCC using 2 mL of plasma was 88.68% (95% CI: 76.97–95.73%), with a specificity of 89.34% (95% CI: 82.47–94.20%), which was greater than the sensitivity of the GALAD score of 58.49% (95% CI: 44.13–71.86%) at the same specificity. When cirrhosis patients were used as controls, the pooled sensitivity of *Qliver* for HCC detection with 1 mL of plasma was still greater than that of the GALAD score, with almost the same specificity (88.06%, 95% CI: 77.82%–94.70% vs. 59.70%, 95% CI: 47.00%–71.51%). For early HCC detection in cirrhosis patients, the sensitivity of *Qliver* for detecting BCLC 0 and A HCC using 1 mL of plasma was significantly greater than that of the GALAD score (72.73%, 95% CI: 39.03%–93.98% vs. 18.18%, 95% CI: 2.28%–51.78%). In previous studies, the GALAD score performed well for detecting any stage of HCC, with a pooled sensitivity, specificity, and AUC of 0.82 (95% CI: 0.78–0.85), 0.89 (95% CI: 0.85–0.91), and 0.92 (95% CI: 0.89–0.94), respectively [2]. The GALAD score for identifying BCLC 0/A HCC has a moderate sensitivity of 0.73 (95% CI: 0.66–0.79) and a high specificity of 0.87 (95% CI: 0.81–0.91) [2]. The performance of the GALAD score in this study appeared to be suboptimal, possibly due to the unofficial configuration of the assay reagents and equipment for AFP, AFP-L3, and DCP compared with that of Roche's Elecsys GALAD assay and the use of plasma instead of serum. Another possible reason may be that most HCC patients in this study had chronic HBV infection, but the GALAD score has a higher sensitivity in the HCC subgroups with HCV or nonviral liver diseases [2]. Therefore, compared with existing surveillance methods, *Qliver* holds great promise for the early detection of HCC caused by HBV infection in the Chinese population, and can supplement the deficiencies of US and AFP in early HCC detection. However, this potential of *Qliver* needs to be further fully validated in a larger population.

In this study, the performance of single methylated genes, *OSR2* and *TSPYL5*, for HCC detection was better than that of single tumor proteins including AFP, AFP-L3 and DCP. Even the performance of the GALAD score when these three proteins were integrated was lower than that of the two single methylated genes. The AUCs of *OSR2* and *TSPYL5* for distinguishing HCC patients from

healthy individuals, cirrhosis patients and patients with benign liver diseases were greater than 0.94 and 0.90, respectively, while those of the GALAD score were less than 0.85. Gene methylation should be more suitable for the early detection of cancer than other biomarkers, such as tumor proteins, ctDNA mutations, copy number variations, and ctDNA fragmentomic features. Hypermethylation of tumor suppressor genes is likely to be the earliest event in carcinogenesis [10], and methylated CpG sites in gene promoter regions are clustered [13]. Therefore, DNA methylation has increased sensitivity for detecting early cancers. The average detection rates of early-stage HCC were only 56.38%, 58.84%, and 33.55%, respectively, using gene methylation, ctDNA mutation and genome-wide cfDNA fragmentation profiles obtained via low-coverage WGS [19]. Although the average detection rate of DNA methylation is not better than that of ctDNA mutations, the detection rate of single gene methylation in early-stage HCC can reach 100%, whereas that of single gene mutations is only 59% [19]. Therefore, identifying methylated genes with excellent performance is very important for early HCC detection.

A meta-analysis of 33 eligible articles from 4113 patients suggested that *RASSF1A* methylation in ctDNA could be used as a potential biomarker for HCC screening, with a sensitivity of 0.644 (95% CI: 0.608–0.678) and a specificity of 0.875 (95% CI: 0.847–0.900) [20]. Oussalah et al. [21] reported that *SEPT9* methylation exhibited high diagnostic accuracy for HCC, with an AUC of 0.944 (95% CI: 0.900–0.970), but the sensitivity was 87.88% (95% CI: 71.8%–96.6%) and the specificity was 67.54% (95% CI: 60.4%–74.1%) when  $\geq 1$  of the triplicate samples was positive. Owing to the heterogeneity of hepatocellular carcinoma, the diagnostic sensitivity of single gene methylation is low. Multitarget panels are expected to improve the sensitivity of HCC detection. Chalasani et al. [22] developed a multitarget panel consisting of four methylated DNAs (*HOXA1*, *EMX1*, *TSPYL5* and *B3GALT6*) and two protein markers (AFP and AFP-L3), which had a high sensitivity of 71% (95% CI: 60%–81%) at 90% specificity for early-stage HCC detection, which was higher than those of the GALAD score (41%, 95% CI: 30–53%) and AFP concentration  $\geq 7.32$  ng/mL (45%, 95% CI: 33–57%). Luo et al. [23] proposed an HCC screening model based on 2321 methylation markers, which achieved 84% sensitivity and 96% specificity in an independent validation cohort with an AUC of 0.934 (95% CI: 0.905–0.963) for distinguishing early-stage HCC patients from high-risk individuals. Xu et al. [12] constructed a model combining 10 CpG sites with a sensitivity of 85.7% and a specificity of 94.3% for detecting HCC in the training dataset and a sensitivity of 83.3% and a specificity of 90.5% in the validation dataset. In this study, only two methylation genes

using 1 mL of plasma were required to achieve an AUC of 0.958 (95% CI: 0.927–0.989) to distinguish HCC patients from cirrhosis patients, with a sensitivity of 72.73% (95% CI: 39.03%–93.98%) and a specificity of 90% for detecting BCLC 0 and A stage HCC. Therefore, *Qliver*, with its low cost, convenient experimental procedures, and superior performance, is more effective for HCC screening compared to targeted sequencing and WGS methods involving hundreds of genes.

The methylation levels of *OSR2* and *TSPYL5* were validated in a variety of tumor cell lines and white blood cells, and the methylation level of the *OSR2* gene in most tumor cell lines was significantly greater than that in white blood cells, especially CAL-62 (thyroid), HCC-2279 (lung), MKN74 (stomach), MKN28 (stomach), EFM-19 (breast) and MCF7 (breast) cells, suggesting that *OSR2* may be a multiple-cancer biomarker. *OSR2* is a mammalian homolog of the *Drosophila* odd-skipped family of transcription factors [24]. *OSR2* methylation has been used to detect other cancers, such as gastric cancer [25] and oropharyngeal squamous cell carcinomas [26]. The methylation level of *OSR2* in HCC primary tumors and recurrent tumors was greater than that in normal solid tissues, and its mRNA expression level was also significantly greater in HCC primary tumors and recurrent HCC tumors than in normal solid tissues, suggesting that *OSR2* may be an oncogene. *OSR2* has been shown to play an important role in cell proliferation and development [27]. Wen et al. [28] provided evidence that *OSR2* promotes prostate cancer tumorigenesis. Han et al. [29] knocked down *OSR2* in human adenocarcinoma (H838) cells and found that cell proliferation was significantly inhibited compared with the non-targeting siRNA group, suggesting that *OSR2* may have an oncogenic role in lung cancer. *TSPYL5*, a member of the nucleosome assembly protein (NAP) superfamily, is likely a tumor suppressor gene in ovarian, lung, and colorectal cancers according to several studies [30, 31]. The higher methylation level but lower mRNA expression in HCC primary tumors and recurrent tumors than in normal solid tissues also supports the role of *TSPYL5* as a tumor suppressor gene. The combination of *OSR2* as an oncogene and *TSPYL5* as a tumor suppressor gene has the potential to detect multiple cancers but requires rigorous and adequate validation.

*Qliver's* potential for HCC prognosis was also explored in this study. By mining the GDC TCGA Liver Cancer (LIHC) 450 K dataset and the GDC TCGA Liver Cancer (LIHC) gene expression RNA-seq dataset, hypermethylated *OSR2* was negatively correlated with the disease-free survival (DFS) of HCC patients ( $p=0.029$ ), and when combined with hypermethylated

*TSPYL5*, this correlation was further increased ( $p=0.008$ ). These findings suggest that *Qliver* has good potential for predicting HCC prognosis, but adequate validation in clinical samples is needed, especially in the Chinese population.

The ideal internal reference genes are stably expressed under any experimental conditions, but many studies have shown that genes stably expressed in different species or under different conditions will change [32]. Therefore, screening appropriate reference genes under specific conditions is highly important. Genes such as *ACTB*, *B2M*, *GAPDH*, 18S rRNA and 28S rRNA are commonly used as internal reference genes in qPCR. However, the stability of these classical reference genes has been questioned in recent years [33, 34]. We found that the MS-qPCR amplification efficiency of *ACTB* was lower than that of highly methylated target genes during technical validation in tissues. This may be because the DNA sequence of *ACTB* is hypomethylated and the bisulfite-converted sequence is AT-rich, which is not conducive to PCR amplification. In this study, we identified for the first time a novel reference gene, *SDF4*, which has a stable high methylation level and high MS-qPCR amplification efficiency compared with *ACTB*, which can improve the diagnostic performance of methylated target genes. We believe that these findings will improve the analytical performance of bisulfite conversion-based MS-qPCR for cancer detection and other applications.

In addition, deconvolution of ctDNA from highly heterogeneous and noisy backgrounds is essential for translating ctDNA methylation data into accurate and effective noninvasive cancer markers. This is especially true for early and/or less aggressive cancers [35]. Lehmann-Werman et al. [36] demonstrated the superior sensitivity of multiple CpG haplotypes in detecting tissue-specific features in ctDNA. Guo et al. [37] used methylated haplotypes for quantitative estimations of tumor load and tissue origin profiles in circulating cell-free DNA from 59 patients with cancer, suggesting that plasma methylated haplotyping is an important tool for the early detection of tumors and their major growth sites and that it is a promising strategy for the early detection of tumors.

This study has several limitations. First, the sample sizes of the Phase 1 plasma cohort and Phase 2 plasma cohort were relatively small, and the inclusion of more patients with early-stage HCC (BCLC stage 0–A) will improve the robustness of the *Qliver* model. Second, although our results were encouraging, they were based on a single-center retrospective case; a prospective multicenter study should be organized to independently validate our findings.

## Conclusions

In this study, we identified two methylated genes, *OSR2* and *TSPYL5*, for HCC detection using a pipeline that included tissue discovery and plasma validation, tissue technical validation and plasma biological validation. A novel reference gene, *SDF4*, was also identified that outperformed *ACTB* in improving the diagnostic performance of the bisulfite-converted MS-qPCR assay of the target methylated genes for cancer detection. An MS-qPCR assay named *Qliver* containing *OSR2*, *TSPYL5* and *SDF4* was subsequently developed and validated for the detection of HCC in an independent plasma cohort. *Qliver* outperformed existing surveillance methods, such as AFP, AFP-L3, DCP and the GALAD score. The potential of *Qliver* in HCC prognosis was also explored in this study, and the analysis of the methylation and mRNA expression databases revealed that it has a strong ability to predict HCC prognosis; however, this finding needs to be fully validated in clinical samples. *OSR2* is highly methylated in many cancer cell lines compared with leukocytes, suggesting that it may be a multicancer biomarker. *Qliver*, which combines a possible oncogene, *OSR2*, and a possible tumor suppressor gene, *TSPYL5*, may have great potential in detecting multiple cancers.

## Abbreviations

HCC	Hepatocellular carcinoma
AFP	Alpha-fetoprotein
AFP-L3	Lens culinaris agglutinin-reactive fraction of AFP
DCP	Des-gamma-carboxyprothrombin
cfDNA	Circulating cell-free DNA
ctDNA	Circulating tumor DNA
MS-qPCR	Methylation-specific quantitative PCR
FFPE	Formalin-fixed paraffin-embedded
gDNA	Genomic DNA
ROC	Receiver operating characteristic curve
AUC	Area under the ROC curve
CI	Confidence interval
GLM	Generalized linear model
TCGA-LIHC	The Cancer Genome Atlas of Liver Hepatocellular Carcinoma
CNGBdb	China National GeneBank DataBase
PPV	Positive predictive value
NPV	Negative predictive value
WBCs	White blood cells
FNH	Focal nodular hyperplasia
HH	Hepatic hemangioma
Cir	Cirrhosis
HCA	Hepatocellular adenoma
HR	Hazard ratio

## Supplementary Information

The online version contains supplementary material available at <https://doi.org/10.1186/s12916-025-04115-w>.

Additional file 1. Table S1-S6. Table S1- [Patient demographics and clinical information included in the development of the Qliver model], Table S2- [Characteristics of the 21 candidate methylation blocks in discovery stage], Table S3- [Comparison of the performance of all HCC Patients with non-HCC subjects], Table S4- [Characteristics of the dual methylation markers and their coefficients in HCC diagnosis], Table S5- [Performances of the Qliver detection model on different subgroups based on clinical

characteristics]. Table S6- [Primer and Probe Sequences used to amplify of *OSR2*, *TSPYL5* and *SDF4*].

Additional file 2. Detailed experimental workflow for HCC methylation biomarker development: from sample processing to gene validation.

Additional file 3. Fig. S1-S6. Fig. S1- [Fig. S1 Visual representation of HCC-specific methylation haplotypes from Targeted Methylation Sequencing. Visual representation of methylation profiles between 43 primary HCC and 32 adjacent normal tissue samples focus on the *OSR2*(A), *KCNKG3*(B), *PITX1*(C), *C1QL4*(D), *IRX5*(E) and *TSPYL5*(F). Each row in the representation signifies the methylation status of a single sample, while each column represents a different CpG locus. The color intensity depicted in the figure corresponds to the different degrees of methylation at these loci]. Fig. S2- [Fig. S2 Visual depictions illustrating the consistent hypermethylation status of *SDF4* across various samples. Visual representation of methylation profiles between 43 primary HCC and 32 adjacent normal tissue samples focus on the Homo sapiens stromal cell-derived factor 4 (*SDF4*). *SDF4* encodes a stromal cell-derived factor belonging to the CREC protein family, identified as the most consistently conserved reference genes in tissues samples from both HCC patients and non-HCC subjects. Each row within the representation signifies the methylation status of an individual sample, while each column represents a distinct CpG locus. The color intensity depicted in the plot corresponds to the varying degrees of methylation at these loci]. Fig. S3- [Fig. S3 Identification of a Novel Reference Gene for MS-qPCR. (A) Heatmap of methylation levels of CpGs in *SDF4* gene for discriminating Primary HCC tumor (n=377), Recurrent HCC tumor (n=2) and Solid Tissue Normal (n=50) in the GDC TCGA Liver Cancer (LIHC) 450 K dataset. (B) ROC curves and associated AUC values with 95% confidential interval for *ZIC4* as target gene which normalized by *ACTB* and *SDF4* reference gene in archived plasma cohort, which consists with 22 HCC, 23 cirrhosis and 23 healthy plasma samples by MS-qPCR. The receiver operating characteristic curve analysis indicated that *SDF4* (AUC=0.826) might be an optimal reference gene for normalization of MS-qPCR data in liver cancer, which show higher HCC detection rate than *ACTB* (AUC=0.786) with p-value 0.06822 use DeLong's test. (C) The distribution of  $\Delta$ CT value of *ACTB* and *SDF4* in archived FFPE samples, which consists with 38 primary HCC tissue and 38 adjacent normal tissue samples. ADJ, adjacent normal tissue; HCC, hepatocellular carcinoma. (D) The distribution of  $\Delta$ CT value of *ACTB* and *SDF4* in archived FFPE samples, which consists with 12 breast cancer and 20 lung cancer tissue samples (p-value were computed with Wilcoxon rank sum test. \*,  $p < 0.05$ ; \*\*,  $p < 0.01$ ; \*\*\*,  $p < 0.001$ ; \*\*\*\*,  $p < 0.0001$ ;  $p > 0.05$  was considered not significant (ns)). (E) Correlation between the CT value of *SDF4* and *ACTB* in WBC DNA (n=7, Spearman's rank correlation rho). (F) Correlation between the CT value of *SDF4* and *ACTB* with DNA input amount in WBC DNA (n=7, Spearman's rank correlation rho). (G) The distribution of methylation levels of CpGs in *SDF4* gene for pancancer tissues in the GDC PanCancer (PANCAN) 450 K dataset.]. Fig. S4- [Fig. S4 Visualization of HCC-specific methylation haplotype of *OSR2* and *TSPYL5* determined by Sanger sequencing. Visualization of methylation haplotype determined by Sanger sequencing within *OSR2* gene in 8 primary HCC and 9 adjacent normal tissue samples (A) and *TSPYL5* (B) gene in 6 primary HCC and 6 adjacent normal tissue samples. These tissues were also used for tissue discovery and tissue technical validation. Allele-specific methylation status from the Sanger data clearly showed that methylated alleles in *OSR2* and *TSPYL5* gene were associated with HCC, highlighting that DNA methylation status in these regions might be a novel biomarker for HCC detection.]. Fig. S5- [Fig. S5 Methylated *OSR2* and *TSPYL5* as Prognostic Biomarkers. The DFS rate of HCC patients from the TCGA 450 K dataset was assessed based on the methylation levels of the *OSR2*(A) and *TSPYL5*(B) genes. Patients with higher methylation levels of *OSR2* or *TSPYL5* gene had a significantly lower DFS rate than those with low methylation levels across different age or AJCC stage. Moreover, combining the *TSPYL5* and *OSR2* genes(C), the DFS rate of HCC patients with high methylation levels of both genes was significantly lower than that of patients with low methylation levels. The findings indicate that the presence of methylated *OSR2* and *TSPYL5* holds promise as prognostic indicators for individuals diagnosed with hepatocellular carcinoma]. Fig. S6- [Fig.

S6 Methylation status of OSR2 and TSPYL5 gene in cancer cell lines and WBCs. For an initial assessment of the methylation status of the OSR2 and TSPYL5 genes, MS-qPCR was performed on cancer cell lines from uterine cancer, leukemia, thyroid cancer, liver cancer, stomach cancer, neuroblastoma, lung cancer, glioma, pancreatic cancer, esophageal squamous cell, colon cancer, ovarian cancer, submandibular, bladder cancer, breast cancer, lymphoma, prostate cancer, glioma, duodenal adenocarcinoma, melanoma, myeloma, teratoma and WBCs. Most of cancer cell lines were either completely or partially methylated in the region of OSR2 gene, highlighting that DNA methylation status in these regions might be a novel biomarker for multiple cancer or pan-cancer detection].

### Acknowledgements

Not applicable.

### Authors' contributions

J.L., L.W., H.Z., W.T., H.L. and H.Y. contributed to the conception and design of the work. W.T., Y.C., F.X., L.Y., M.W. and F.K. collected samples and clinical information. H.L., H.Y., L.X., A.Z., L.Z., J.B., Y.W. and F.S. conducted data analysis and interpretation; W.T., H.L. and H.Y. drafted the manuscript. J.L., L.W. and H.Z. reviewed the data and revised the manuscript. All authors read and approved the final manuscript.

### Funding

This study was sponsored by the Natural Science Foundation of Fujian Province (2023J05234, 2023J011297), Joint Funds for the Innovation of Science and Technology, Fujian province (2021Y9232, 2021Y9227, 2024Y9620), high level talents training project of Fujian Cancer Hospital (2022YNG01), and Young and Middle-aged Scientific Research Major Project of Fujian Provincial Health Commission (2022ZQNZD009).

### Data availability

The original contributions data presented in the current study are included in the manuscript/supplementary material; further inquiries are available from the corresponding author upon reasonable request. The 450K methylation, mRNA expression and survival data were downloaded from UCSC Xena Hub repository, <https://xenabrowser.net/>. Targeted bisulfite sequencing data from the tissue discovery cohorts were deposited into the Sequence Read Archive (SRA) under accession number SRP577656, <https://www.ncbi.nlm.nih.gov/sra/SRP577656>.

### Declarations

#### Ethics approval and consent to participate

All procedures were approved by Medical Ethics Committee of the Fujian Cancer Hospital (K2022-103-01). All research was conducted in accordance with the Declarations of Helsinki. Written consent was obtained from all subjects.

#### Consent for publication

Not applicable.

#### Competing interests

The authors declare no competing interests.

#### Author details

<sup>1</sup>Department of Hepatopancreatobiliary Surgery, Clinical Oncology School of Fujian Medical University, Fujian Cancer Hospital, Fuzhou, China. <sup>2</sup>Fujian Provincial Key Laboratory of Tumor Biotherapy, Clinical Oncology School of Fujian Medical University, Fujian Cancer Hospital, Fuzhou, China. <sup>3</sup>Berry Oncology Corporation, Beijing, China. <sup>4</sup>Fujian Key Laboratory of Advanced Technology for Cancer Screening and Early Diagnosis, Fuzhou, China. <sup>5</sup>Genetrix Biotech Corporation, Beijing, China. <sup>6</sup>Department of Medical Oncology, Clinical Oncology School of Fujian Medical University, Fujian Cancer Hospital, Fuzhou, China.

Received: 24 July 2024 Accepted: 1 May 2025

Published online: 12 May 2025

### References

- Bray F, Laversanne M, Sung H, Ferlay J, Siegel RL, Soerjomataram I, et al. Global cancer statistics 2022: GLOBOCAN estimates of incidence and mortality worldwide for 36 cancers in 185 countries. *CA Cancer J Clin*. 2024;74(3):229–63.
- Guan MC, Zhang SY, Ding Q, Li N, Fu TT, Zhang GX, et al. The performance of GALAD score for diagnosing hepatocellular carcinoma in patients with chronic liver diseases: a systematic review and meta-analysis. *J Clin Med*. 2023;12(3): 949.
- Singal AG, Pillai A, Tiro J. Early detection, curative treatment, and survival rates for hepatocellular carcinoma surveillance in patients with cirrhosis: a meta-analysis. *PLoS Med*. 2014;11(4): e1001624.
- Tzartzeva K, Obi J, Rich NE, Parikh ND, Marrero JA, Yopp A, et al. Surveillance imaging and alpha fetoprotein for early detection of hepatocellular carcinoma in patients with cirrhosis: a meta-analysis. *Gastroenterology*. 2018;154(6):1706–1718.e1.
- Esfef JM, Hajifathalian K, Ansari-Gilani K. Sensitivity of ultrasound in detecting hepatocellular carcinoma in obese patients compared to explant pathology as the gold standard. *Clin Mol Hepatol*. 2020;26(1):54–9.
- Ayoub WS, Steggerda J, Yang JD, Kuo A, Sundaram V, Lu SC. Current status of hepatocellular carcinoma detection: screening strategies and novel biomarkers. *Ther Adv Med Oncol*. 2019;11: 1758835919869120.
- Yang JD, Addissie BD, Mara KC, Harmsen WS, Dai J, Zhang N, et al. GALAD score for hepatocellular carcinoma detection in comparison with liver ultrasound and proposal of GALADUS score. *Cancer Epidemiol Biomarkers Prev*. 2019;28(3):531–8.
- Jones PA. Functions of DNA methylation: islands, start sites, gene bodies and beyond. *Nat Rev Genet*. 2012;13(7):484–92.
- Hata T, Dal Molin M, Hong SM, Tamura K, Suenaga M, Yu J, et al. Predicting the grade of dysplasia of pancreatic cystic neoplasms using cyst fluid DNA methylation markers. *Clin Cancer Res*. 2017;23(14):3935–44.
- Newsham I, Sendera M, Jammula SG, Samarajiva SA. Early detection and diagnosis of cancer with interpretable machine learning to uncover cancer-specific DNA methylation patterns. *Biol Methods Protoc*. 2024;9(1):bpae028.
- Aucamp J, Bronkhorst AJ, Badenhorst CPS, Pretorius PJ. The diverse origins of circulating cell-free DNA in the human body: a critical re-evaluation of the literature. *Biol Rev Camb Philos Soc*. 2018;93(3):1649–83.
- Xu RH, Wei W, Krawczyk M, Wang W, Luo H, Flagg K, et al. Circulating tumour DNA methylation markers for diagnosis and prognosis of hepatocellular carcinoma. *Nat Mater*. 2017;16(11):1155–61.
- Lakshminarasimhan R, Liang G. The role of DNA methylation in cancer. *Adv Exp Med Biol*. 2016;945:151–72.
- Guo P, Zheng H, Li Y, Li Y, Xiao Y, Zheng J, et al. Hepatocellular carcinoma detection via targeted enzymatic methyl sequencing of plasma cell-free DNA. *Clin Epigenetics*. 2023;15(1):2.
- Kim SC, Kim DW, Cho EJ, Lee JY, Kim J, Kwon C, et al. A circulating cell-free DNA methylation signature for the detection of hepatocellular carcinoma. *Mol Cancer*. 2023;22(1):164.
- Hajian-Tilaki K. Sample size estimation in diagnostic test studies of biomedical informatics. *J Biomed Inform*. 2014;48:193–204.
- Fan R, Chen L, Zhao S, Yang H, Li Z, Qian Y, et al. Novel, high accuracy models for hepatocellular carcinoma prediction based on longitudinal data and cell-free DNA signatures. *J Hepatol*. 2023;79(4):933–44.
- Siegel RL, Miller KD, Wagle NS, Jemal A. Cancer statistics, 2023. *CA Cancer J Clin*. 2023;73(1):17–48.
- Manea I, Iacob R, Iacob S, Cerban R, Dima S, Oniscu G, et al. Liquid biopsy for early detection of hepatocellular carcinoma. *Front Med (Lausanne)*. 2023;10:1218705.
- Zhang Z, Chen P, Xie H, Cao P. Using circulating tumor DNA as a novel biomarker to screen and diagnose hepatocellular carcinoma: a systematic review and meta-analysis. *Cancer Med*. 2020;9(4):1349–64.
- Oussalah A, Rischer S, Bensenane M, Conroy G, Filhine-Tresarrieu P, Debard R, et al. Plasma mSEPT9: a novel circulating cell-free DNA-based epigenetic biomarker to diagnose hepatocellular carcinoma. *EBioMedicine*. 2018;30:138–47.
- Chalasanani NP, Ramasubramanian TS, Bhattacharya A, Olson MC, Edwards VDK, Roberts LR, et al. A novel blood-based panel of methylated DNA and protein markers for detection of early-stage hepatocellular carcinoma. *Clin Gastroenterol Hepatol*. 2021;19(12):2597–2605.e4.

23. Luo B, Ma F, Liu H, Hu J, Rao L, Liu C, et al. Cell-free DNA methylation markers for differential diagnosis of hepatocellular carcinoma. *BMC Med.* 2022;20(1):8.
24. Lan Y, Ovitt CE, Cho ES, Maltby KM, Wang Q, Jiang R. Odd-skipped related 2 (*Osr2*) encodes a key intrinsic regulator of secondary palate growth and morphogenesis. *Development.* 2004;131(13):3207–16.
25. Li WH, Zhou ZJ, Huang TH, Guo K, Chen W, Wang Y, et al. Detection of *OSR2*, *VAV3*, and *PPFIA3* methylation in the serum of patients with gastric cancer. *Dis Markers.* 2016;2016:5780538.
26. Kostareli E, Holzinger D, Bogatyrova O, Hielscher T, Wichmann G, Keck M, et al. HPV-related methylation signature predicts survival in oropharyngeal squamous cell carcinomas. *J Clin Invest.* 2013;123(6):2488–501.
27. Kawai S, Abiko Y, Amano A. Odd-skipped related 2 regulates genes related to proliferation and development. *Biochem Biophys Res Commun.* 2010;398(2):184–90.
28. Wen P, Lei H, Deng H, Deng S, Rodriguez Tirado C, Wang M, et al. *Hyd/UBR5* defines a tumor suppressor pathway that links Polycomb repressive complex to regulated protein degradation in tissue growth control and tumorigenesis. *Genes Dev.* 2024;38(13–14):675–91.
29. Han Q, Fernandez J, Rajczewski AT, Kono TJY, Weirath NA, Rahim A, et al. A multi-omics study of epigenetic changes in type II alveolar cells of A/J mice exposed to environmental tobacco smoke. *Int J Mol Sci.* 2024;25(17): 9365.
30. Huang C, He C, Ruan P, Zhou R. *TSPYL5* activates endoplasmic reticulum stress to inhibit cell proliferation, migration and invasion in colorectal cancer. *Oncol Rep.* 2020;44(2):449–56.
31. Huang C, Ruan P, He C, Zhou R. *TSPYL5* inhibits the tumorigenesis of colorectal cancer cells in vivo by triggering DNA damage. *J Cancer Res Ther.* 2023;19(4):898–903.
32. Ferreira MJ, Silva J, Pinto SC, Coimbra S. I choose you: selecting accurate reference genes for qPCR expression analysis in reproductive tissues in *Arabidopsis thaliana*. *Biomolecules.* 2023;13(3): 463.
33. Ahn HR, Baek GO, Yoon MG, Son JA, You D, Yoon JH, et al. *HMBS* is the most suitable reference gene for RT-qPCR in human HCC tissues and blood samples. *Oncol Lett.* 2021;22(5):791.
34. Gao Q, Wang XY, Fan J, Qiu SJ, Zhou J, Shi YH, et al. Selection of reference genes for real-time PCR in human hepatocellular carcinoma tissues. *J Cancer Res Clin Oncol.* 2008;134(9):979–86.
35. Hong S, Lin B, Xu M, Zhang Q, Huo Z, Su M, et al. Cell-free DNA methylation biomarker for the diagnosis of papillary thyroid carcinoma. *EBio-Medicine.* 2023;90: 104497.
36. Lehmann-Werman R, Neiman D, Zemmour H, Moss J, Magenheimer J, Vaknin-Dembinsky A, et al. Identification of tissue-specific cell death using methylation patterns of circulating DNA. *Proc Natl Acad Sci U S A.* 2016;113(13):E1826–34.
37. Guo S, Diep D, Plongthongkum N, Fung HL, Zhang K, Zhang K. Identification of methylation haplotype blocks aids in deconvolution of heterogeneous tissue samples and tumor tissue-of-origin mapping from plasma DNA. *Nat Genet.* 2017;49(4):635–42.

## Publisher's Note

Springer Nature remains neutral with regard to jurisdictional claims in published maps and institutional affiliations.